Available online at www.sciencedirect.com
SCIENCE DIRECT®
PERGAMON
International Journal of Heat and Mass Transfer 46 (2003) 3897–3907
International Journal of HEAT and MASS TRANSFER
www.elsevier.com/locate/ijhmt

Bubble nucleation on micro line heaters under steady or finite pulse of voltage input

Jung-Yeul Jung, Jung-Yeop Lee, Hong-Chul Park, Ho-Young Kwak *

Department of Mechanical Engineering, Chung-Ang University, Seoul 156-756, South Korea

Received 27 August 2002; received in revised form 22 February 2003

Abstract

Nucleation temperatures on micro line heaters under steady voltage input were measured precisely by obtaining the *I–R* (current–resistance) characteristic curves of the heaters having dimensions of 50 μm in length, 3 or 5 μm in width, and 0.583 μm in thickness. The bubble nucleation temperature on the heater with 3 μm width is higher than the superheat limit, while the temperature on the heater with broader width of 5 μm is considerably less than the superheat limit. The nucleation temperature under a finite voltage pulse input was also measured for 5-μm width heater. The nucleation temperatures were also estimated by using the molecular cluster model for bubble nucleation on the cavity free surface with effect of contact angle. The bubble nucleation process was observed by a microscope/35 mm camera unit with a flash light of μs duration.

1. Introduction

Device miniaturization evolved from IC-based micro-fabrication technology has increased the importance of understanding fluid flow in micro-channel and phase change in micro-geometry. One of the promising methods for designing micro-actuators is the use of volume expansion due to phase change of a trapped liquid [1], because the volume expansion created by the phase change with low power input can generate relatively large forces. In fact, bubble nucleation on micro-heaters, which has been successfully employed for bubble jet printers [2], can be used for the bubble-powered micro-actuators [3]. However, nucleation and growth process in the micro-heaters must be studied additionally, and the nucleated bubble depending on the input current to the heater must be controlled to properly design and operate bubble-powered micro-actuators.

Avedisian et al. [4] measured the bubble nucleation temperature on a micro-scale metal heater, which is currently used in commercial bubble jet printers, with the bridge circuit and dynamic amplifier. The largest heating rate and the highest nucleation temperature measured on the heater immersed in a pool of water were about 0.25×10^9 °C/s and 560 K respectively. Also they found that the bubble nucleation temperature on the heater increases as the heating rate increases and the highest nucleation temperature of 560 K is almost the same as that obtained from the molecular cluster model for bubble nucleation [5] with an appropriate nucleation rate corresponding to the heating rate of the heater. Recently Tsai and Lin [6] investigated the transient bubble formation on the micro-heater with size of $100 \times 10 \times 0.5$ μm^3 by using various values of constant electrical current input and found that the higher electrical current generated bubble faster at a higher temperature.

In this study, bubble nucleation and growth on micro line heaters under steady or transient voltage input were investigated experimentally and theoretically. Two types of micro-heaters 3 and 5 μm wide, respectively, 50 μm long and 0.523 μm thick were used. Dielectric liquids such as FC-72, FC-77 and FC-40 were used as working fluids. DC voltage to the heaters was increased in 0.01–0.1 V increment to obtain *I–R* (current–resistance)

* Corresponding author. Tel.: +82-2-820-5278; fax: +82-2-826-7464.
E-mail address: kwakhy@cau.ac.kr (H.-Y. Kwak).

0017-9310/03/$ - see front matter
doi:10.1016/S0017-9310(03)00189-3

Nomenclature

A_s	heater area
C_p	heat capacity of polysilicon heater (700 J/kg °C)
F_n	free energy needed to form n-mer cluster
h	convection heat transfer coefficient (284 W/m^2/°C)
J_i	current density
J_n	nucleation rate of n-mer cluster per unit volume
J_s	nucleation rate per unit area
k_B	Boltzmann constant
k_p	conductivity of polysilicon heater (34 W/m/°C)
k_s	conductivity of silicon dioxide layer (1.4 W/m/°C)
L	heater length
m	mass of molecule
n	number of molecules in a cluster
N	number density
P_v	vapor pressure
P_∞	ambient pressure
R	gas constant
R_p	resistance of heater
s	thickness of silicon dioxide layer
T	temperature of liquid
T_f	melting temperature of liquid
T_s	superheat limit of liquid
T_∞	ambient temperature of liquid
V_m	effective molecular volume of liquid
w	heater width
z_h	heater thickness
Z	coordination number

Greek symbols

α_p	heat diffusivity in polysilicon heater
β	accommodation coefficient
ΔH_{vap}	enthalpy of evaporation
ΔH_f	enthalpy of fusion
ε_m	energy needed to separate a pair of molecules
ξ	temperature coefficient of resistivity (0.0012 °C)
ρ_0	resistivity of polysilicon heater (7.42×10^{-6} Ωm)
ρ_p	density of polysilicon heater (2.32×10^3 kg/m^3)

Subscript

c	critical cluster or critical size bubble

characteristic curves for the heaters by steady voltage input, from where was the temperature for bubble nucleation deduced. The nucleation temperature in the 5-μm width heater applied with a finite voltage pulses of 100–200 μs was also measured. Bubble nucleation was also observed by using a microscope/35 mm camera unit with μs duration flash light. Also the temperatures for the incipient bubble nucleation were estimated by using the molecular cluster model [5,6] for bubble formation.

2. A vapor bubble formation model based on molecular interactions

In the molecular cluster model of vapor bubble formation, the surface energy needed to form the critical cluster grounded at the molecular level is utilized while the kinetic formalism of the classical theory of nucleation is kept. In this model, the chemical potential difference between saturated and metastable liquid molecules is assumed to drive the clustering of activated molecules.

Employing the assumptions mentioned above, Kwak and Panton [5] obtained the stability condition for the critical cluster and the corresponding free energy for bubble formation. These are

$$-(P_\infty - P_v)n_c^{1/3} = \frac{Z\varepsilon_m}{3}\Big/ V_m \tag{1}$$

$$F_{nc} = \frac{Z\varepsilon_m}{6} n_c^{2/3} \tag{2}$$

The energy to separate a pair of molecules ε_m given in Eqs. (1) and (2) can be obtained when molecular properties such as ionization potential, polarizability, and van der Waals' diameter of molecule are provided. In ideal liquid model [7], each molecule is surrounded by a certain number of molecules at an equal distance. Each molecule yields the average coordination number (Z) of 11. Thus, the face-centered cubic lattice structure having the coordination number of 12 is considered a reasonable model for liquid structure. If any cluster, an aggregate of the liquid molecules in the metastable state, meets the stability condition, the molecules in the cluster ceases to interact and vaporize spontaneously.

Using the kinetic theory argument analogous to the condensation case they also obtained the steady state nucleation per unit volume. Using the minimum free energy for the formation of the critical cluster, Eq. (2), we can obtain the nucleation rate of the critical cluster, J_{nc} (nuclei/cm^3 s),

$$J_{nc} = \beta N \left(\frac{k_B T}{2\pi m}\right)^{1/2} \left[\frac{Z}{18\pi}\left(\frac{\varepsilon_m}{k_B T}\right)\right]^{1/2} 4\pi \left(\frac{3V_m}{4\pi}\right)^{2/3} \cdot \exp\left[-\frac{\Delta H_{vap}}{RT} - \frac{\Delta H_f}{RT_f}\right] \cdot N \cdot \exp\left[-\frac{Z}{6}\left(\frac{\varepsilon_m}{k_B T}\right) n_c^{2/3}\right] \quad (3)$$

Eq. (3) gives n_c for any given nucleation rate of the critical cluster, J_{nc}. Once n_c and the molecular properties are known, vapor pressure P_v and the corresponding superheat limit can be found from Eq. (1). Using a nucleation rate of $J_{nc} = 10^{22}$ clusters/cm^3 s, this modified cluster model can well predict the superheat limits of liquids, such as various hydrocarbons, as well as the evaporation process at the limit [8]. Note that the limit measured by the droplet explosion technique [9] is about 90% of the critical temperatures of liquids at atmospheric pressure. The molecular cluster model discussed above suggests that evaporation of molecules rather than bubble formation takes place at the superheat limit, as confirmed by experiment [10].

When the liquid contacts a solid surface with no cavity, the nucleation temperature may be obtained by considering the contact angle and is given by the following equation [11].

$$T = \frac{F_{nc}\Phi}{k_B} \Big/ \left[\ln \frac{CN^{-1/3}(\eta/\Phi^{1/2})}{J_s}\right] \quad (4)$$

where C is the pre-exponential factor in Eq. (3), and the factors Φ and η, which account for the volume and surface area truncation, respectively, of the bubble due to the contact angle [11,12], are given as

$$\eta = \tfrac{1}{2}(1 + \cos\theta) \quad (5)$$

$$\Phi = \tfrac{1}{4}(1 + \cos\theta)^2(2 - \cos\theta) \quad (6)$$

The surface nucleation rate may be obtained by using the following equation [4].

$$J_s = \frac{1}{A_s}\left|\frac{d(F_n/k_B T)}{dT}\right| \dot{T} \quad (7)$$

where $\dot{T}$ is the measured heating rate, which is about 5×10^7 °C/s for the micro line heater used in this study. The corresponding nucleation rate of the micro line heater used is about 10^{13}/cm^2 s.

3. Micro line heater

3.1. Experimental apparatus and procedures

Two types of micro line heater have been designed and fabricated by using the standard IC process [13]. The polysilicon heaters fabricated on the 0.8 μm silicon dioxide layer with P-type prime wafer have same length of 50 ± 0.1 μm and thickness of 0.523 ± 0.004 μm and two different widths of 3 ± 0.1 and 5 ± 0.1 μm. No cavity was found on the micro line heaters fabricated when we inspected them with a microscope and CCD camera. Two driving pads, which connected with the line heater electrically, have dimensions of 100×100 μm^2. The pads were made by depositing 0.7-μm thick aluminum film on the polysilicon pads. Schematic and enlarged views of the micro line heater on the silicon wafer are shown in Fig. 1.

A pressure tight test chamber made of acryl is shown in Fig. 2(a). The inner dimensions of the chamber, which holds the working fluid, are $30 \times 30 \times 10$ mm^3. Two 4 mm OD copper tubes that provide current to the heater as well as working fluid to the chamber were connected to the probe tips in the chamber through the wall. Two tungsten probe tips, which have a 25 μm diameter end, contacted the aluminum film pads. The other ends of diameter 0.5 mm were forced to contact with the copper tube inside the chamber as shown in Fig. 2(b).

Fluorinert liquids, such as FC-72, FC-77 and FC-40, were used as working fluids. Methanol and ethanol were not appropriate as working fluid to the polysilicon heater. In fact, when methanol or ethanol wetted the heater, the heater became damaged permanently or the resistance of the heater became infinity.

The bubble nucleation temperature under steady voltage input can be measured. A DC-voltage current standard (Yokogawa 2553) was used to supply current to the heater. The current and voltage to the heater were monitored simultaneously. Calculated heater resistances obtained by measuring current and voltages were also

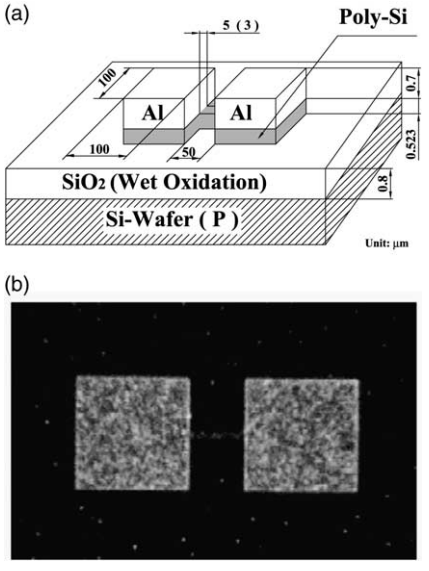

Fig. 1. Schematic (a) and enlarged (b) view of micro line heater.

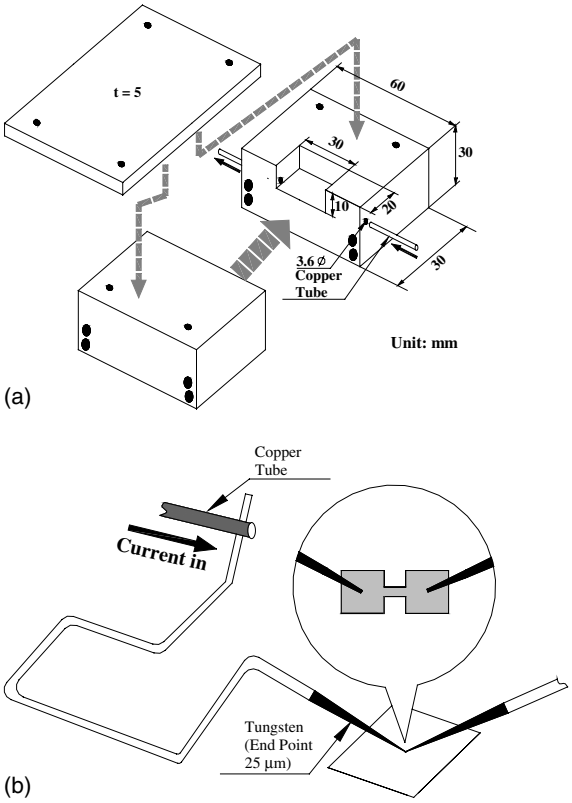

Fig. 2. Schematic of acryl chamber and tungsten probe tip contacting on driving pads.

compared to the values obtained directly. DC voltage to the heater was increased by 0.1 V increment to obtain the current–resistance (I–R) characteristic curve for each heater–liquid combination, and this curve was used to deduce the temperature for bubble nucleation on the heater–liquid system. The voltage was increased in a smaller increment of 0.01 V near the nucleation point to measure the bubble nucleation temperature accurately. At each interval, we waited for about 10 s to see possible bubble formation.

The resistance change of the micro-heater applied with a finite voltage pulse of 100–200 μs can be measured by the following method. Shown schematically in Fig. 3, a Wheatstone bridge circuit can measure the change in the resistance along the micro line heater while a current pulse is applied. The Wheatstone bridge consists of four resistors R_2, R_3, R_4 and R_h, of which resistors R_2 and R_3 have same fixed value of 4.7 Ω. The resistance R_4 was varied depending on the applied voltage to the bridge circuit. The test heater was in the lower right part of the bridge circuit and was labeled R_h. The magnitude of DC voltage applied between the top and bottom of the bridge was provided by a DC-voltage current standard (Yokokawa 2553). The pulse width of the input voltage was controlled by a delay generator (SRS DG535), which actuates the MOSFET driver (IRF530) shown in the bottom of the circuit. The voltage difference $(V_d - V_b)$ to appear across the middle of the bridge was amplified by AD847 amplifier and was measured by an oscilloscope.

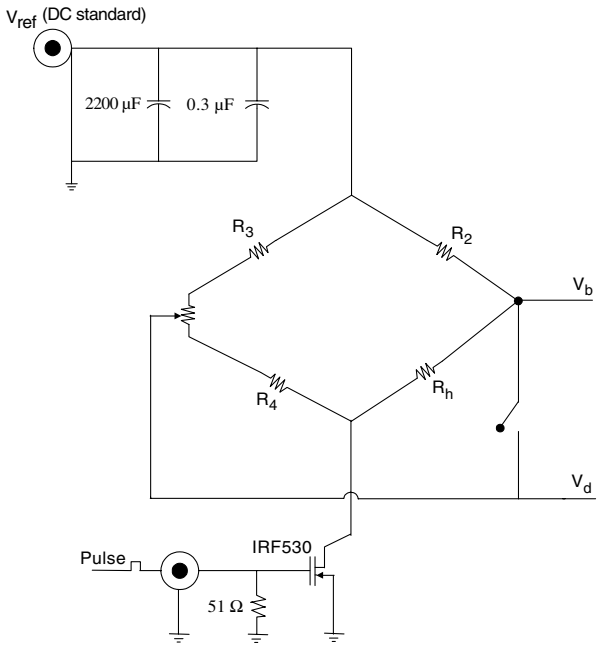

Fig. 3. Schematic of a Wheatstone bridge circuit employed.

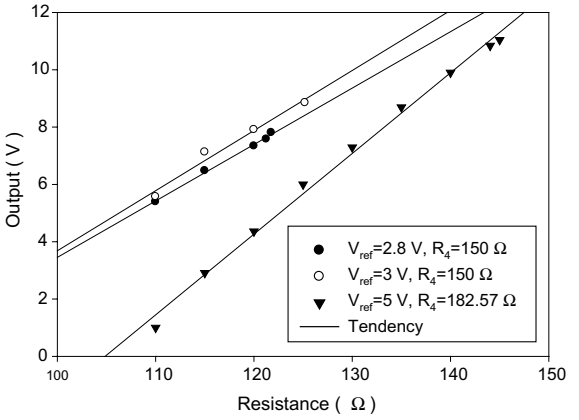

Fig. 4. Output voltage from the bridge circuit with known resistors of R_h.

For a given input voltage of V_{ref} and proper value of R_4, the output voltages for different resistance values of R_h are shown in Fig. 4. For these measurements, known values of resistors were used. The measured output voltage was linearly dependent on the value of the resistance, R_h. These results shown in Fig. 4 were used in the calibration of the time dependent resistance of the polysilicon micro line heater.

Bubble nucleation was also observed by using a microscope-CCD camera or microscope-35 mm camera unit with a flash unit (Palflash 501) of μs duration.

3.2. A model for micro line heaters

A heater starts when a current is applied through the two driving pads, which are larger than the heater. The silicon substrate beneath the silicon dioxide layer acts as a heat sink because conduction heat transfer plays a very important role in removing the heat dissipation in the micro line heater [13]. For example, when the temperature at the hottest point of heater of dimensions $50 \times 5 \times 0.53$ μm^3 is 160.1 °C, the heater consumes 58.5 mW. In this case, without nucleate boiling, the heat flow rate from the heater to the driving pad and to the silicon substrate beneath the heater are 7.5 and 51.0 mW, respectively. The heat fluxes corresponding to the heat flow rates are 1.30×10^9 and 2.0×10^8 W/m^2, respectively, which are comparable with the heat flux, 6.0×10^9 W/m^2, achieved at the absolute evaporation rates of FC-72 at the same temperature. Since the heat flux of evaporation on the micro-heater calculated to be less than 10^8 W/m^2, large heat flows to the substrate.

Applying the principle of conservation energy to the differential element in the heater, one may obtain the following heat diffusion equation for the heater [13].

$$\frac{\partial^2 T}{\partial x^2} = \frac{1}{\alpha_p}\frac{\partial T}{\partial t} + \varepsilon(T - T_r) \tag{8}$$

where,

$$\alpha_p = \frac{k_p}{C_p \rho_p} \tag{9.1}$$

$$\varepsilon = \frac{k_s}{k_p}\frac{1}{z_h s} + \frac{h}{k_p}\left(\frac{1}{z_h} + \frac{2}{w}\right) - \frac{J_i^2 \rho_0 \xi}{k_p} \tag{9.2}$$

$$T_r = T_\infty + \frac{J_i^2 \rho_0}{k_p \xi} \tag{9.3}$$

where the first and second terms in ε represent the ratio of the conductive and convective outflows to the conductive inflow in the heater element, respectively, and the last term represents the ratio of heat dissipation to the conductive inflow in the heater element. T_r in Eq. (9.3) denotes the temperature increase due to heat dissipation in the heater element.

The steady state solution of Eq. (8) at the following initial and boundary conditions can be obtained.

Initial condition:

$$T(x, t = 0) = T_\infty \tag{10.1}$$

Boundary conditions:

$$T(x = 0, t) = T_\infty, \quad T(x = L, t) = T_\infty \tag{10.2}$$

The temperature distribution along the line heater at steady state is given by [14]

$$T(x) = T_r - \frac{J_i^2 \rho_0}{k_p \varepsilon}\frac{\cosh\left[\sqrt{\varepsilon}(x - L/2)\right]}{\cosh\left[\sqrt{\varepsilon}(L/2)\right]} \tag{11}$$

The resistance of the heater can be obtained by considering the power dissipation in the heater. That is

$$R = \int_0^L \mathrm{d}R(T) = \frac{\rho_0 L}{w z_h}\left[1 + \xi(\overline{T} - T_\infty)\right] \tag{12}$$

where $\overline{T}$ is the average temperature of the line heater and is given by

$$\overline{T} = \frac{1}{L}\int_0^L T\,\mathrm{d}x = T_r - (T_r - T_\infty)\tanh\left(\frac{\sqrt{\varepsilon}}{2}L\right)\Big/\frac{\sqrt{\varepsilon}}{2}L \tag{13}$$

Of course, the theoretical solutions of the heat diffusion equation for the micro line heater and the resistance heater at steady state given in Eqs. (11) and (12), respectively, were obtained by assuming that both ends of the line heater remain at ambient temperature during heating. This assumption was confirmed to be reasonable by a finite element analysis [13,14]. However, large heat flows from heater to the pads because of the large temperature gradient at the boundary [15]. Therefore, the nucleation temperature was determined by fitting the

theoretical I–R curve to the measured I–R curve by adjusting the values of properties of polysilicon heater, such as ρ_0 and ζ. This procedure, which is a key element in this study, is crucial in measuring the correct temperature for bubble nucleation on the heater.

The transient solution of the heat diffusion equation can also be obtained with the method of separation variables [16]. The final result is given by

$$T(s,t) = T_\infty + 2(T_r + T_\infty)\exp[-\alpha_p \varepsilon t]\sum_{n=1}^{\infty}\frac{1}{n\pi}[1-(-1)^n] \times \frac{1}{1+((n\pi)/(\sqrt{\varepsilon}L))^2}\sin\left(\frac{n\pi x}{L}\right) \times \exp\left[-\alpha_p t\left(\frac{n\pi}{L}\right)^2\right] \quad (14)$$

The instantaneous average temperature of the heater can be obtained by integrating Eq. (14) along the heater, as follows:

$$\overline{T}(t) = T_\infty + 8(T_r - T_\infty)\exp[-\alpha_p \varepsilon t]\sum_{n=1}^{\infty}\left[\frac{1}{(2n+1)\pi}\right]^2 \times \frac{1}{1+[((2n+1)\pi)/(\sqrt{\varepsilon}L)]^2} \times \exp\left\{-\alpha_p t\left[\frac{(2n+1)\pi}{L}\right]^2\right\} \quad (15)$$

where these transient solutions given in Eqs. (14) and (15) at $t = 0$ represent the steady state solution given in Eqs. (11) and (13), respectively. With help of Eqs. (12) and (15), one can estimate the instantaneous average temperature of the heater by measuring the instantaneous electrical resistance along the heater.

4. Results and discussion

4.1. A case of steady voltage input

Measured I–R characteristic curve up to the bubble nucleation point for the 5-μm width heater in FC-72 when a steady voltage was supplied is shown in Fig. 5. The corresponding theoretical I–R curve which is fitted closely to the measured one by adjusting the variables such as polysilicon resistivity ($\rho_0 = 6.09 \times 10^{-4}$ Ω cm) and its temperature coefficient ($\xi = 0.80 \times 10^{-3}$/°C), is also shown in Fig. 5. Hardly one can obtain such closely fitted curves by adjusting the variables related to the heat transfer mechanism [14]. With these adjust values of ρ_0 and ξ, one can obtain the accurate nucleation temperature, which is shown in Fig. 6. Heaters of different widths produced drastically different nucleation temperatures, respectively. For the 3-μm width heater, the bubble nucleation temperature 430.4 K is certainly greater than the superheat limit of FC-72, 421.0 K by 9.4 °C. On the other hand, for the 5-μm width heater, the nucleation temperature 389.7 K is less than the superheat limit by as much as 31.3 °C, at which heterogeneous nucleation might take place.

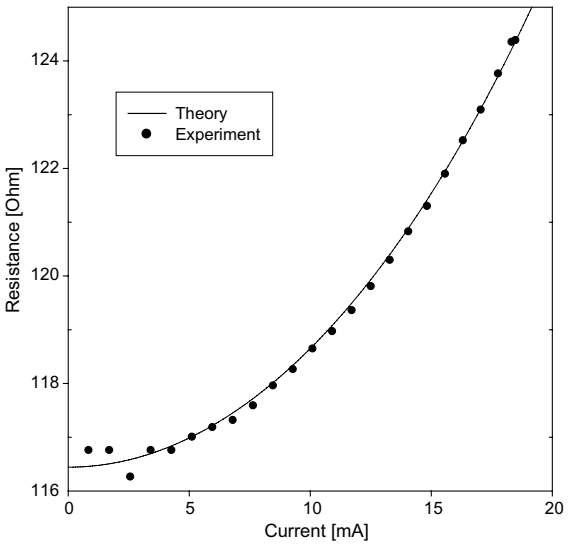

Fig. 5. Calculated (—) and experimental (●) I–R characteristics for the polysilicon heater of $50 \times 5 \times 0.523$ μm^3 in FC-72. The theoretical characteristics was obtained with $\rho_0 = 6.09 \times 10^{-4}$ Ω cm and $\xi = 0.80 \times 10^{-3}$/°C.

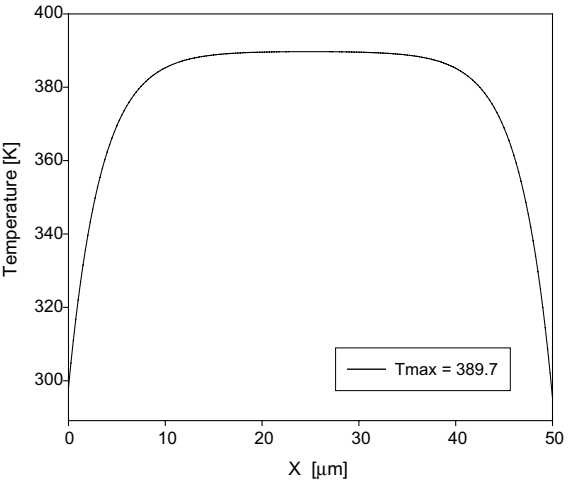

Fig. 6. Steady state temperature distribution along the 5-μm width line heater at the current of 18.34 mA.

Same experiment was done with other fluorinerts such as FC-77 and FC-40 and similar results were obtained. The measured nucleation temperatures, superheat limit calculated by the molecular cluster model [5,8], and the thermodynamic limit estimated by the Berthelot equation of state [17] are given in Table 1. The

Table 1
Measured nucleation temperature for different heater widths in various fluorinerts and the liquid superheat limits estimated theoretically

Liquids	Heater width (μm)	Measured nucleation temperature (K)	Superheat limit, T_s (K)	Adjusted resistivity[a], ρ_0 (Ω cm)/and temperature coefficient, ξ (/°C)
FC-72	3	430.4	421.0 (414.6[b])	$5.90\times10^{-4}/0.75\times10^{-3}$
	5	389.7		$6.09\times10^{-4}/0.80\times10^{-3}$
FC-77	3	467.8	465.2 (458.7[b])	$5.90\times10^{-4}/0.78\times10^{-3}$
	5	424.5		$6.11\times10^{-4}/0.79\times10^{-3}$
FC-40	3	515.7	500.8 (499.2[b])	$5.91\times10^{-4}/0.80\times10^{-3}$
	5	464.2		$6.09\times10^{-4}/0.84\times10^{-3}$

[a] Listed values of resistivity and temperature coefficient for polysilicon are 7.5×10^{-4} Ω cm and 1.2×10^{-3}/°C respectively [13].
[b] Calculated from the Berthelot equation of state.

nucleation rates employed in this calculation are $J_{n_c}=10^{22}$, 10^{21} and 10^{20} nuclei/cm^3 s for FC-72, FC-77 and FC-40, respectively. The adjusted values of resistivity and its temperature coefficient for liquid–heater combinations to obtain the nucleation temperature are also given in Table 1. The resistivity and its temperature coefficient values changed slightly, depending on the liquid–heater combinations employed.

The uncertainty in the width of heater of ±0.1 μm yields substantial error of ±20 °C for the measured nucleation temperature in the 1-μm width heater; of ±10.0 °C in the 3-μm width heater; but of ±2.0 °C in the 5-μm width heater. Also the heater temperature was very sensitive to the input current for such narrow-width heaters; for example, a 0.5 mA increase in the current yielded 30.0 °C increase in heater temperature by the 1-μm width heater. This is a reason why we did not use 1-μm width heater in this experiment. The uncertainty in the thickness of heater, ±0.004 μm was taken as the tolerance of α-Step equipment. The uncertainty in the current to the heater, ±0.05 mA yielded error of ±1.0 °C, so that the total uncertainty in the measurement of the nucleation temperature in the 3-μm width heater is about ±12 °C. The total uncertainty in the measurement of the nucleation temperature in the 5-μm width heater is only ±3 °C under the same uncertainty in the variables concerned.

However, the comparison of electrical resistance between measurement and the calculation values by the relation $R=\rho_0 L/(wz_h)$ at the ambient temperature provides us the dimensions of heater, 50 μm × 3.1 μm × 0.527 μm for 3-μm width heater and 49.9 μm × 5.1 μm × 0.527 μm for 5-μm width heater. The estimated nucleation temperatures with these dimensions of the heaters, which are listed in Table 1, reduce error in the measurement of heater temperature considerably. Even when the error is taken into account in the nucleation temperature measurement, bubble nucleation on the 3-μm width heater was found to occur above the superheat limit of liquid. The measured temperatures of bubble nucleation on the 2-μm width heater in three different Fluorinert liquids (FC-43, FC-75, and FC-72) are even close to the critical temperatures of individual liquids [14]. This observation indicates that enough volume of liquid evaporated is needed for bubble formation so that thinner width heater needs higher nucleation temperature and consequently sufficient evaporated volume for nucleation [15].

Apparently, heterogeneous nucleation even on a cavity free surface takes place on the 5-μm width heater. With the nucleation rate of 10^{11}–10^{13}/cm^2 s, the nucleation temperatures depending on contact angle, which are obtained by Eq. (4) are shown in Fig. 7. With a contact angle of 110°, which is considered reasonable for such well wetted liquids, the nucleation temperature agreed well with the measured values as shown in Table 1. However, the factors given in Eqs. (5) and (6) which greatly affect the nucleation temperature are determined

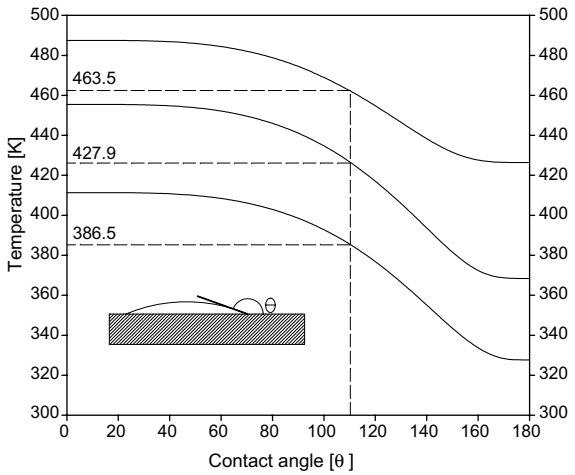

Fig. 7. Predicted nucleation temperature with contact angle for FC-72, FC-77, and FC-40 with the nucleation rate values of 10^{13}, 10^{12}, and 10^{11}/cm^2 s respectively.

empirically [11]. No proper method to estimate the contact angle of vapor on a plane surface is available at present, although a type of molecular interaction at liquid/liquid and liquid/solid interface was proposed [18]. Note that the minimum surface temperature required for bubble formation in water on a 65 μm × 65 μm heater element used in commercial thermal ink-jet printers is about 178.9 °C [4], which is also certainly far below the superheat limit of water while the highest nucleation temperature measured was 560 K at the heating rate of 0.25×10^9 °C/s. One may obtain the homogeneous superheat limit at the contact angle of 0°, as shown in Table 1. Indeed, at the contact angle of 40°, which is well within the range of water–metal combination, the temperature of the bubble nucleation on the micro square heater by Eq. (4) with a nucleation rate of $J_s = 10^{13}/\text{cm}^2\,\text{s}$ is close to the measured value of 560 K.

For the cases shown in Fig. 7, appropriate nucleation rate values were employed to obtain smooth nucleation temperature curve up to the boiling point. The nucleation rate values are $10^{13}/\text{cm}^2\,\text{s}$ for FC-72, $10^{12}/\text{cm}^2\,\text{s}$ for FC-77 and $10^{11}/\text{cm}^2\,\text{s}$ for FC-40. Note that the ionization potential for the fluorinerts, which are not available at present, were estimated so that the nucleation temperature at the contact angle of 180° becomes the boiling point of liquid as shown in Fig. 7, which was suggested by Avedisian [4]. The polarizability of working fluids was obtained by Lorentz–Lorenz formula [19]. The temperature dependence of the saturated liquid density and the effective diameter of the molecules were estimated by the Gunn–Yamada [20] method. To estimate the vapor pressure dependence on pressure, a corresponding-states formula by Dong and Linhard [21] was employed.

4.2. A case of finite voltage pulse input

Fig. 8 shows time dependent voltage measured from the bridge circuit during the application of input voltage pulse whose magnitude and duration are 2.8 V and 200 μs, respectively, to the micro line heater. The polysilicon heater employed as a resistor for R_h in this case worked normally after 0.28 μs from the start of voltage application. The resistance of the micro-heater after the voltage application increases at first as shown in Fig. 8. After this increase, sudden decrease and subsequent increase in the resistance occurs. It turns out that such abnormal behavior in the resistance measurement is due to the source signal of the IRF 530 used in this experiment.

The instantaneous temperature of the heater during the application of the voltage pulse can be calculated with the data that appear in Fig. 4 by the following procedure: with a steady-state output voltage value, the corresponding resistance value of the heater can be obtained with the calibrated data shown in Fig. 4. With

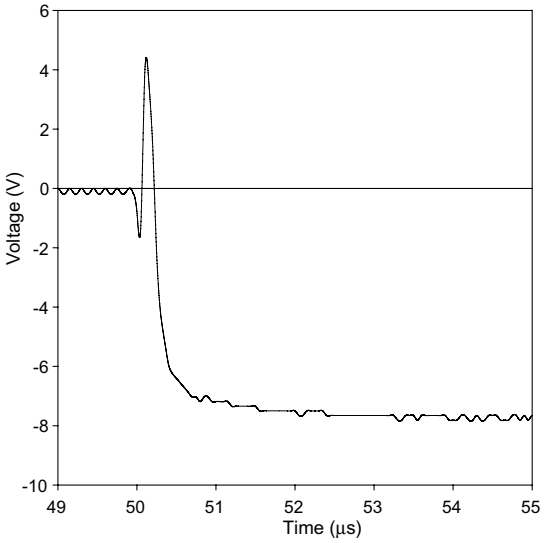

Fig. 8. Voltage output from the bridge circuit with a polysilicon line heater applied with a voltage of 2.8 V for 200 μs.

this resistance value of the heater at steady state, one can calculate the average temperature of the micro line heater and then corresponding input current to the heater at steady state by using Eqs. (11) and (12), respectively. Then one can obtain the instantaneous average temperature of the heater by using Eq. (15) with this value of the input current. The measured instantaneous temperature of the heater can also be obtained with the given input voltage, the time dependent output voltage data from the bridge, and the value of the resistor, R_4. The time dependent values of the resistance along the micro line heater, values which can be obtained from the calibrated data shown in Fig. 4, yield the measured instantaneous average temperature.

Using the procedure described above, the measured and calculated values of the instantaneous temperature of the polysilicon heater applied with a voltage of 2.8 V for 200 μs is shown in Fig. 9(a). Even though the time needed to reach steady state, which is about 2.5–3 μs, is similar in both cases, the temperature rise observed in the heater at the initial stage is steeper compared to the gradual increase in the calculation result. When the minimum input voltage of 2.8 V needed for bubble growth is applied, the average temperature achieved in the heater at the steady state is about 420.7 K, which is close to the superheat limit of 420.1 K calculated by the molecular cluster model [8] for bubble nucleation. As shown in Fig. 9(b), slight increase in the voltage (3 V) magnitude produced 11 °C increase in the heater temperature. As confirmed in Fig. 11, bubble growth started at 30 μs after applying the voltage pulse for this case. On the other hand, as shown in Fig. 10, the observed and calculated temperature obtained with the application of

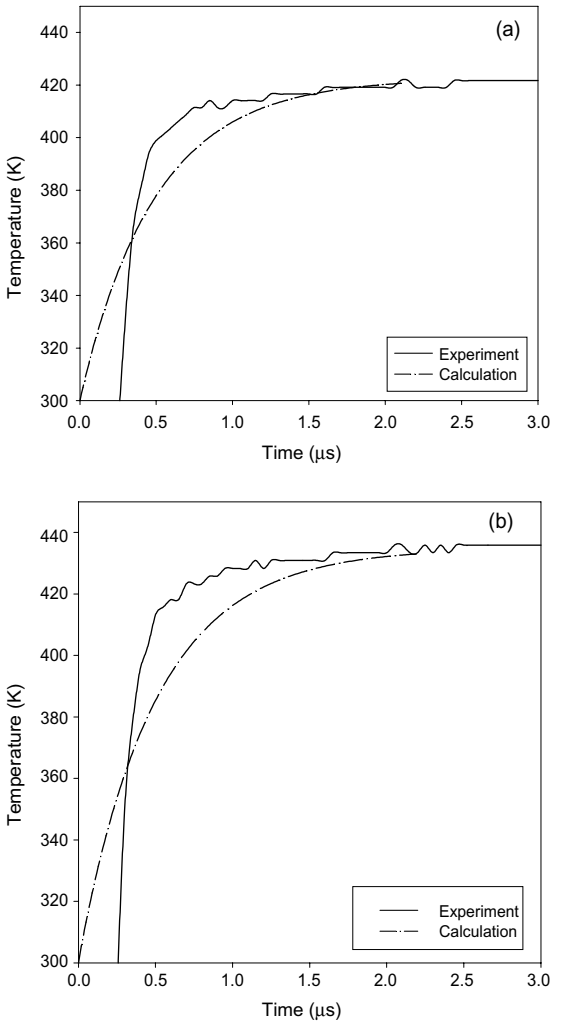

Fig. 9. Calculated and measured temperature changes on a polysilicon line heater applied with voltages of 2.8 V (a) and 3.0 V (b) for 200 μs.

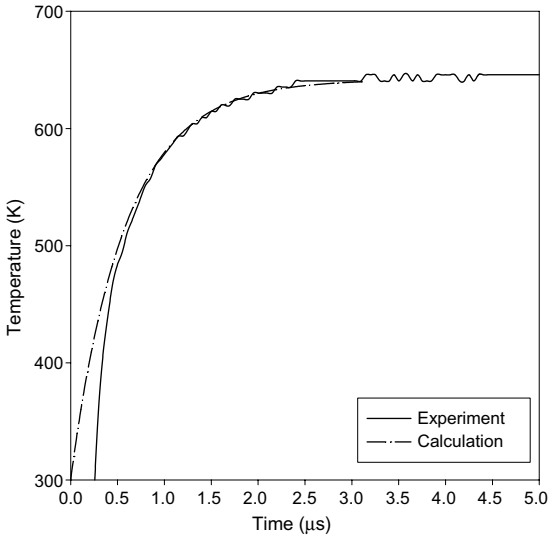

Fig. 10. Calculated and measured temperature changes on a polysilicon line heater applied with a voltage of 5.0 V for 200 μs.

a rather high voltage of 5.0 V for 200 μs duration agreed well. However, the temperature of the heater achieved at the steady state is as much as 650 K, which is much higher than the superheat limit of FC-72, 420 K. In this case, only 5 μs was needed for a bubble to start growing after applying voltage pulse.

For the case of moderate input voltage of 3 V, bubble nucleation growth and subsequent collapse processes were visualized when the voltage pulse of 100 μs was applied as shown in Fig. 11(a). The bubble continued to grow until heat supply to the heater stopped. After the heat supply to the heater discontinued, the bubble started to decrease in size and finally collapsed. The period of growth was almost the same as that of collapse. As clearly seen in first two frames of Fig. 11(a) and (b), when a spherical bubble formed from the spheroidal shape of superheated liquid layer above the heater, the bubble dimension shrank because the evaporated liquid which covered the heater broadly accumulated to become a bubble. This finding suggests that a bubble can form on the micro line heater if enough liquid volume above the heater evaporated [14]. When the pulse duration increases at the fixed input voltage of 3.0 V, the growth period increases and the maximum size of the bubble become larger as shown in Fig. 11(b). Certainly the period of collapse from the maximum size bubble becomes longer if the duration of input voltage is longer, so that the growth and subsequent collapse period and the maximum size of the bubble can be controlled by the magnitude and duration of the input voltage to the micro line heater. No bubble departure can be found with this moderate input voltage of 3 V for the line heater. For the case of high input voltage of 4 V, as shown in Fig. 12, bubble grew at 5 μs after applying voltage pulse. This growth can be explained by the fact that enough evaporated volume for bubble growing forms in very short time at much higher surface temperature of the heater than the superheat limit of liquid.

Finally it should be noted that transient bubble formation behavior observed by Tsai and Lin [6] was not found in this study. They found that a bubble was nucleated on the micro-heater 2 s after applying moderate input current while the wall temperature dropped up to 8 °C depending on the magnitude of input current. Such temperature drop phenomenon during bubble nucleation was also observed on the rather large square heater of 50–100 μm [22] and was treated analytically [23]. A notable characteristic related to this phenomenon is that the wall superheat for bubble nucleation is rather small,

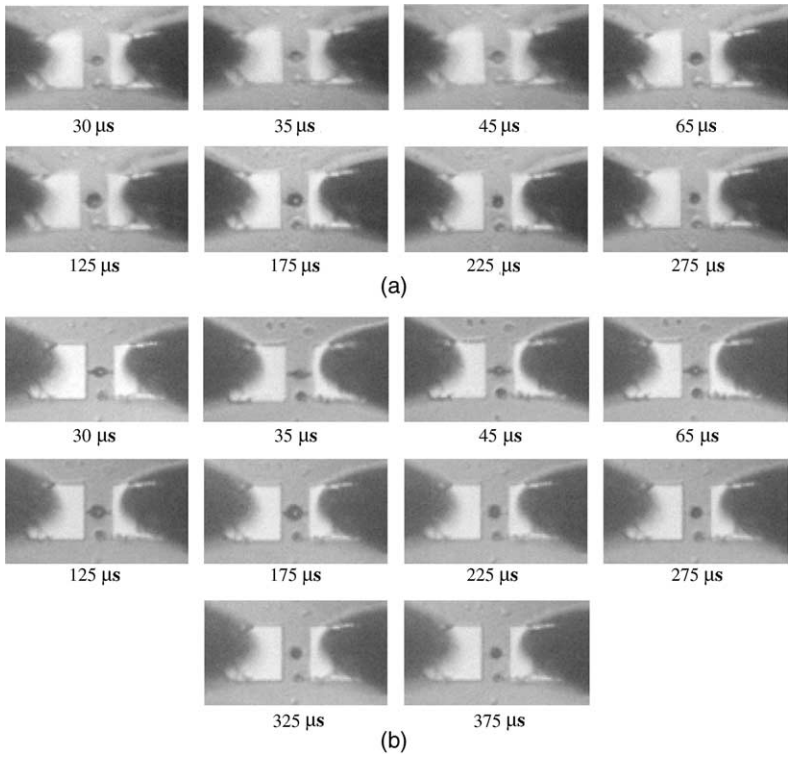

Fig. 11. Bubble growth and collapse on a micro line heater applied with a voltage of 3.0 V with pulse of 100 μs (a) and 200 μs (b).

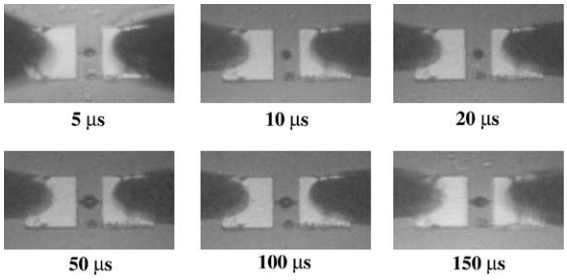

Fig. 12. Bubble growth and collapse on a micro line heater applied with a voltage of 4.0 V with pulse of 100 μs.

which was typically observed in macroscopic boiling [24]. It is concluded that nucleation temperature as well as nucleation process depend crucially on the heater size.

5. Conclusion

The bubble nucleation temperatures on the micro line heater under steady voltage were measured precisely by obtaining the *I–R* characteristic curves of the heater. The nucleation temperature on the 3-μm width heater was higher than the superheat limit estimated by molecular cluster model for bubble nucleation by 6–10 °C, which could be also predicted by analytically. On the other hand, the activation temperature for nucleation on the 5-μm width heater was considerably less than the superheat limit of liquid, where heterogeneous nucleation may occur. The measured temperature for the heterogeneous bubble nucleation were in close agreement with the values estimated by using the molecular cluster model as applied to a surface with appropriate value of contact angle. The nucleation temperature under a finite voltage pulse was also measured for 5-μm width heater. The minimum temperature for bubble nucleation in FC-72 with the application of a 200 μs voltage pulse was measured to be 421 K, which is close to the superheat limit of FC-72. Bubble size and the period of growth on the micro line heater can be controlled by the magnitude and duration of the applied voltage pulse.

Acknowledgements

This work has been supported by the grants from Korean Science and Engineering Foundation under Contract 1999-1-304-002-5.

References

[1] J. Ji, L.J. Chaney, M. Kaviany, P.L. Bergstrom, K.D. Wise, Microactuation based on thermally-driven phase

change, in: Digest IEEE International Conference on Solid-State Sensors and Actuators, 1991, pp. 1037–1040.
[2] N.J. Nielson, History of thermaljet printerhead development, HP J. 36 (5) (1985) 12–13.
[3] L. Lin, A.P. Pisano, Thermal bubble powered microactuators, Microsyst. Technol. 1 (1994) 51–58.
[4] C.T. Avedisian, W.S. Osborne, F.E. McLeod, C.M. Curley, Measuring bubble nucleation temperature on the surface of a rapidly heated thermal inkjet heater immersed in a pool of water, Proc. R. Soc. London A 455 (1999) 3875–3899.
[5] H. Kwak, R.L. Panton, Tensile strength of simple liquids predicted by a molecular interaction model, J. Phys. D: Appl. Phys. 18 (1985) 647–659.
[6] J. Tsai, L. Lin, Transient thermal bubble formation on polysilicon micro-resistors, Trans. ASME: J. Heat Transfer 124 (2002) 375–382.
[7] J.D. Bernal, The structure of liquids, Sci. Am. 203 (August) (1960) 125–134.
[8] H. Kwak, S. Lee, Homogeneous bubble nucleation predicted by a molecular interaction model, Trans. ASME: J. Heat Transfer 113 (1991) 714–721.
[9] M. Blander, J. Katz, Bubble nucleation in liquids, AIChE J. 21 (1975) 833–848.
[10] J.E. Shepherd, E. Sturtevant, Rapid evaporation at the superheat limit, J. Fluid Mech. 121 (1982) 379–402.
[11] C.T. Avedisian, Modeling homogeneous bubble nucleation in liquids, in: Modeling of Engineering Heat Transfer Phenomena, Computational Mechanics, London, 1998, (Chapter 11).
[12] S.J.D. Van Stralen, R. Cole, Boiling Phenomena, vol. 1, McGraw-Hill, 1979.
[13] L. Lin, A.P. Pisano, Bubble forming on micro line heater, Micromec. Sens. Actuat. Syst. DSC-32 (1991) 147–163.
[14] L. Lin, A.P. Pisano, V.P. Carey, Thermal bubble formation on polysilicon micro resistors, Trans. ASME: J. Heat Transfer 20 (1998) 735–742.
[15] S. Oh, S. Seung, H. Kwak, A model of bubble nucleation on a micro line heater, Trans. ASME: J. Heat Transfer 121 (1999) 220–225.
[16] C.H. Mastrangelo, Thermal applications of microbridges, Ph.D. thesis, U.C. Berkeley, USA, 1990.
[17] J.G. Eberhart, H.C. Schnyders, Application of the mechanical stability condition to the prediction of the limit of superheat for normal alkanes, ether, and water, J. Phys. Chem. 77 (1973) 2730–2736.
[18] F.M. Fowkes, Attractive forces at interfaces, Ind. Eng. Chem. 56 (1964) 40–52.
[19] M. Born, E. Wolf, Principles of Optics, Pergamon, Oxford, 1975.
[20] R.D. Gunn, T. Yamada, A corresponding states correlation of saturated liquid volumes, AIChE J. 17 (1971) 1341–1345.
[21] W.-G. Dong, J.H. Lienhard, Corresponding states correlation of saturated and metastable properties, Can. J. Chem. Eng. 64 (1986) 158–161.
[22] S. Takagi, N. Yamamoto, T. Inoue, K. Hijikata, Behavior of a boiling bubble from a micro-scale heater, in: Proceedings of the 11th International Heat Transfer Conference, vol. 2, 1998, pp. 479–484.
[23] I. Sekine, Temperature fluctuation under bubble of nucleation pool boiling: experiment and proposal of a new factor of evaporation, in: Proceedings of the Fourth JSME-KSME Thermal Engineering Conference, vol. 1, 2000, pp. 409–414.
[24] M.G. Cooper, A.J.P. Lloyd, The microlayer in nucleate pool boiling, Int. J. Heat Mass Transfer 12 (1969) 895–913.